ELSEVIER

Smad3 Deficiency Leads to Mandibular Condyle Degradation via the Sphingosine 1-Phosphate (S1P)/S1P₃ Signaling Axis

Q17 Q2 Hiroki Mori, Takashi Izawa, and Eiji Tanaka

From the Department of Orthodontics and Dentofacial Orthopedics, Institute of Biomedical Sciences, Tokushima University Graduate School, Tokushima, Japan

Temporomandibular joint osteoarthritis is a degenerative disease that is characterized by permanent cartilage destruction. Transforming growth factor (TGF)-β is one of the most abundant cytokines in the bone matrix and is shown to regulate the migration of osteoprogenitor cells. It is hypothesized that TGF-β/Smad3 signaling affects cartilage homeostasis by influencing sphingosine 1-phosphate (S1P)/ S1P receptor signaling and chondrocyte migration. We therefore investigated the molecular mechanisms by which crosstalk may occur between TGF-β/Smad3 and S1P/S1P receptor signaling to maintain condylar cartilage and to prevent temporomandibular joint osteoarthritis. Abnormalities in the condylar subchondral bone, including dynamic changes in bone mineral density and microstructure, were observed in $Smad3^{-/-}$ mice by microcomputed tomography. Cell-free regions and proteoglycan loss characterized the cartilage degradation present, and increased numbers of apoptotic chondrocytes and matrix metalloproteinase 13^+ chondrocytes were also detected. Furthermore, expression of S1P receptor 3 (S1P₃), but not S1P₁ or S1P₂, was significantly down-regulated in the condylar cartilage of $Smad3^{-/-}$ mice. By using RNA interference technology and pharmacologic tools, S1P was found to transactivate Smad3 in an S1P₃/TGF-β type II receptor-dependent manner, and S1P₃ was found to be required for TGF-β—induced migration of chondrocyte cells and downstream signal transduction via Rac1, RhoA, and Cdc42. Taken together, these results indicate that the Smad3/S1P₃ signaling pathway plays an important role in the pathogenesis of temporomandibular joint osteoarthritis. (Am J Pathol 2015, 185: 1—15; http://dx.doi.org/10.1016/j.ajpath.2015.06.015)

Q5 Temporomandibular disorder is an orofacial disease that refers to a number of clinical problems that involve the masticatory musculature, the temporomandibular joint (TMJ), and associated structures.[1] Osteoarthritis (OA) is a severe pathologic change that often affects the TMJ of patients with severe temporomandibular disorder and is characterized by progressive cartilage degradation and subchondral bone changes.[2,3] Despite extensive studies of the pathogenesis of cartilage degradation in OA, current therapies are unable to impede or reverse histopathologic progression to advanced OA.[4] Low bone mineral density and abnormal bone turnover were identified in the early stages of OA in the knee joint.[5] These results suggest that abnormal subchondral bone remodeling plays an important role in the pathogenesis of OA in the knee. The TMJ is one of the most common sites for OA,[3,6] and emerging evidence indicates that abnormal remodeling of mandibular condylar subchondral bone occurs during the early stages of TMJ-OA.[7–9] Thus, subchondral bone may have a causative role in TMJ-OA disorder. In the mandibular condyle, subchondral bone is mainly formed by endochondral ossification, and this process is regulated by factors that are endogenously expressed by chondrocytes.[10] However, the cause and effect relation between subchondral bone abnormalities and the development of TMJ-OA has not yet been established. Furthermore, it is hypothesized that the accumulation of

chondroprogenitor cells at injury sites is due to the migration of these cells from the surrounding matrix. Nevertheless, the physiologic and/or pathologic functions of chondroprogenitor cells and their migratory effects on healing in TMJ-OA joints remain unknown.

Transforming growth factor (TGF)-β is one of the most abundant cytokines in the bone matrix[11] and is shown to play a central role in the remodeling of bone by regulating the migration, proliferation, and differentiation of osteoprogenitor cells.[12,13] Cytokine signaling is transduced via a heteromeric complex of two types of transmembrane serine/threonine kinase receptors that phosphorylate receptor-activated Smad proteins. Correspondingly, an osteoarthritic phenotype is observed in mice that express a dominant-negative TGF-β type II receptor (TGF-βRII) and in mice with systemic ablation of Smad3,[14] a key effector of TGF-β signaling. The long-lasting action exerted by the TGF-β/Smad3 signaling pathway implies that a complex cascade of transcriptional events is involved, and the mechanistic details are not fully characterized. Several studies have reported that some of the effects elicited by the TGF-β/Smad3 signaling pathway are transmitted via a pathway initiated by activation of sphingosine kinase (Sphk), followed by intracellular generation of the bioactive lipid, sphingosine 1-phosphate (S1P).[15] Once formed, S1P can serve as an extracellular ligand for five distinct membrane receptors (termed $S1P_{1-5}$) or as an intracellular mediator.[16] As a result, S1P is involved in regulating vital functions such as cell migration, inflammation, angiogenesis, and wound healing.[17–19]

Here, we hypothesize that TGF-β/Smad3 signaling influences cartilage homeostasis by influencing S1P/S1P receptor signaling and chondrocyte migration. To test this hypothesis, mandibular chondrocyte cells were isolated from $Smad3^{-/-}$ mice, and the expression profile of the $S1P_{1-5}$ receptors was investigated. In addition, the effects of Smad3 and S1P on chondrocyte cell migration and proteoglycan degradation in mandibular condylar cartilage were investigated.

Materials and Methods

Mice

$Smad3^{-/-}$ mice were previously generated by deleting exon 8 of $Smad3$ by homologous recombination.[20] Litters from mated pairs of mice heterozygous for the targeted deletion of $Smad3$ on a mixed 129/C57B6 background were used in the present study. PCR genotyping of the $Smad3^{-/-}$ mice was performed as previously described.[20] Both $Smad3^{-/-}$ and wild-type (WT) mice were maintained under specific pathogen-free conditions and were analyzed in this study.[21] This study was approved by the Ethics Committee of Tokushima University for Animal Research (approval 12134).

Micro-CT

Mandibles were resected from 4-month-old mice. The mandibles were free of soft tissues and were fixed overnight in 70% ethanol. The bones were then analyzed by high-resolution microcomputed tomography (micro-CT; SkyScan 1176 scanner and CTAn software version 1.15; Bruker, Billerica, MA). Briefly, image acquisition was performed at 50 kV and 200 μA. During scanning, the samples were enclosed in tightly fitting plastic wrap to prevent movement and dehydration. Thresholding was applied to the images to segment the bone from the background. Two-dimensional images were used to generate three-dimensional (3D) renderings with the use of the 3D Creator software CTVox version 3.0 (Bruker) supplied with the instrument. The resolution of the micro-CT images is 9 μm per pixel. The microstructural variables analyzed included the bone volume-to-trabecular volume ratio, trabecular thickness, and trabecular separation.

Tissue Preparation and Histologic Staining

TMJ tissues were removed and fixed in 4% freshly prepared paraformaldehyde with EDTA in phosphate-buffered saline (PBS) for 20 days. With the use of a microtome (Carl Zeiss HM360, Jena, Germany), serial sagittal sections were cut from paraffin-embedded TMJ tissue blocks. Serial sections of each condyle were stained with hematoxylin and eosin for histologic assessment, 0.1% safranin-O, and 0.02% fast green to detect cartilage and proteins, respectively, and toluidine blue to detect proteoglycans. Tartrate-resistant acid phosphatase staining was used to identify osteoclasts according to the manufacturer's instructions (387-A; Sigma-Aldrich, St. Louis, MO).

Histologic Analysis

A modified Mankin scoring system[22] was used to assess the degree of cartilage degeneration. Safranin-O—stained sections were used to score samples for features of cartilage disease, including changes in cellularity, structural abnormalities, and uptake of safranin-O as a measure of glycosaminoglycan distribution and loss. The sections were analyzed by three independent experts who were blinded to the type of samples analyzed.

Immunohistochemistry

After the deparaffinization and blocking of sections, immunohistochemistry was performed with various primary antibodies. Briefly, sections were incubated with primary rabbit polyclonal antibodies that recognized phospho (p)-Smad3, type II collagen (Col2a1), aggrecan, matrix metallopeptidase (MMP)-13, MMP-9, Sphk1, $S1P_3$, type X collagen (Col10a1; Abcam, Cambridge, United Kingdom), cleaved caspase-3, caspase-9 (Cell Signaling Technology, Danvers, MA), or $S1P_1$ (Cayman Chemical, Ann Arbor, MI) diluted in PBS that contained 0.1% bovine serum albumin overnight at 4°C. The

sections were then washed in PBS and were incubated with corresponding secondary antibodies at room temperature. After 1 hour, antibody binding was visualized by staining with 3,3-diaminobenzidine (2.5 mg/mL), followed by counterstaining with Mayer's hematoxylin. Control sections were incubated with nonimmune (control) IgG antibodies. All of the stained sections were mounted and analyzed with a BioRevo BZ-9000 microscope (KEYENCE, Osaka, Japan).

TUNEL Staining

The distribution of apoptotic chondrocyte cells was assessed with the TdT-mediated dUTP-digoxigenin nick-end labeling (TUNEL) method, which specifically labels the 3′-hydroxyl terminus of DNA strand breaks. TUNEL staining was performed with an Apoptosis *In Situ* Detection Kit (Wako Pure Chemical, Osaka, Japan), according to the manufacturer's directions. Negative controls were stained with TdT substrate solution without TdT. TUNEL⁺ apoptotic cells were observed by microscopy (KEYENCE).

RNA Extraction and Real-Time PCR

Total RNA was extracted from mandibular condylar cartilage with the use of Nucleo Spin RNA II kits (Macherey-Nagel, Duren, Germany) according to the manufacturer's instructions. RNA concentrations were estimated with a NanoDropND-2000 (Nano Drop Technologies, Wilmington, DE). Total RNA was converted to cDNA with the use of a High-Capacity RNA to c-DNA Kit (Applied Biosystems, Foster City, CA) according to the manufacturer's instructions. PCR amplifications were then performed for each reaction mix that contained cDNA, primers, and PowerSYBR Green PCR Master Mix (Applied Biosystems). mRNA levels of Smad3, Sphk1, $S1P_{1-5}$, MMP-9, MMP-13, aggrecan, Col2a1, Sox9, osteocalcin, type I collagen, and Col10a1 were measured by a 7500 Real-Time PCR system (Applied Biosystems). All quantitations were normalized to an endogenous control, glyceraldehyde 3-phosphate dehydrogenase, and were calculated according to the comparative cycle threshold method (ΔΔCt). The following primers were used: $S1P_1$, 5′-CGCAGTTCTG-AGAAGTCTCTGG-3′ (sense) and 5′-GGATGTCACAG-GTCTTCGCCTT-3′ (antisense); $S1P_2$, 5′-TGTTGCTGG-TCCTCAGACGCTA-3′ (sense) and 5′-AGTGGGCTTTG-TAGAGGACAGG-3′ (antisense); $S1P_3$, 5′-GCTTCATCGT-CTTGGAGAACCTG-3′ (sense) and 5′-CAGAGAGCCA-AGTTGCCGATGA-3′ (antisense); $S1P_4$, 5′-GTGTATGGC-TGCATCGGTCTGT-3′ (sense) and 5′-GAGCACATAG-CCCTTGGAGTAG-3′ (antisense); $S1P_5$, 5′-AGACTCCTC-CAACAGCTTGCAG-3′ (sense) and 5′-TAGAGCTGCG-ATCCAAGGTTGG-3′ (antisense); Sphk1, 5′-GCTTCTGT-GAACCACTATGCTGG-3′ (sense) and 5′-ACTGAGCACA-GAATAGAGCCGC-3′ (antisense); MMP-13, 5′-GATGA-CCTGTCTGAGGAAGACC-3′ (sense) and 5′-GCATTTCT-CGGAGCCTGTCAAC-3′ (antisense); MMP-9, 5′-GCTGA-CTACGATAAGGACGGCA-3′ (sense) and 5′-TAGTGGT-GCAGGCAGAGTAGGA-3′ (antisense); aggrecan, 5′-CAG-GCTATGAGCAGTGTGATGC-3′ (sense) and 5′-GCTGC-TGTCTTTGTCACCCACA-3′ (antisense); Col2a1, 5′-GCT-GGTGAAGAAGGCAAACGAG-3′ (sense) and 5′-CCATC-TTGACCTGGGAATCCAC-3′ (antisense); Sox9, 5′-AGTA-CCCGCATCTGCACAAC-3′ (sense) and 5′-ACGAAGG-GTCTCTTCTCGCT-3′ (antisense); osteocalcin, 5′-CAGCG-GCCCTGAGTCTGA-3′ (sense) and 5′-GCCGGAGTCTG-TTCACTACCTTA-3′ (antisense); type I collagen, 5′-GAG-CGGAGAGTACTGGATCG-3′ (sense) and 5′-GTTAGG-GCTGATGTACCAGT-3′ (antisense); Col10a1, 5′-GTACC-AAACGCCCACAGGCATA-3′ (sense) and 5′-GGACC-AGGAATGCCTTGTTCTC-3′ (antisense); glyceraldehyde 3-phosphate dehydrogenase, 5′-AGGTCGGTGTGAACG-GATTTG-3′ (sense) and 5′-TGTAGACCATGTAGTTGAG-GTCA-3′ (antisense).

Immunoblot Analysis

Total protein was extracted from primary chondrocyte cells isolated from mandibular condylar cartilage in a lysis buffer composed of 10 mmol/L Tris-HCl (pH 7.4), 150 mmol/L NaCl, 5 mmol/L EDTA, 1% SDS, 10 mg/mL aprotinin, 50 mg/mL leupeptin, and 1 mmol/L phenylmethanesulfonyl fluoride. After centrifugation, supernatant fluids were collected, and whole lysate protein concentrations were determined by using BCA Protein Assay Reagent (Thermo Fisher Scientific, Rockford, IL). Equal amounts of lysates in 2× Laemmli sample buffer were resolved by 8% to 12% SDS-PAGE at 85 V for 2 hours. Separated proteins were subsequently transferred electrophoretically onto polyvinylidene difluoride membranes. The membranes were blocked with 0.1% Tween 20−Tris-buffered saline that contained 5% skim milk at room temperature. After 1 hour, primary rabbit polyclonal antibodies that recognized MMP-13, Col2a1, p-Smad3, S1P₃, Sphk1, TGF-βRII, Col10a1 (Abcam), p-extracellular signal-regulated kinase (ERK), p-Akt, p-p38, cleaved caspase-3, cleaved caspase-9 (Cell Signaling Technology), S1P₁ (Cayman Chemical), or Sox-9 (Santa Cruz Biotechnology, Santa Cruz, CA) were added as appropriate (each diluted 1:1000), and the membranes were incubated overnight at 4°C. Levels of β-actin were detected as a loading control with the use of a mouse monoclonal antibody (Sigma-Aldrich) in 0.1% Tween 20−Tris-buffered saline (dilution 1:5000). Membranes were subsequently washed with 0.1% Tween 20−Tris-buffered saline (15 minutes, 3×) and then were incubated for 1 hour with the appropriate secondary antimouse (Millipore, Billerica, MA) or anti-rabbit (Cell Signaling) antibodies conjugated to horseradish peroxidase. Bound antibodies were visualized by using the LumiGLO Western blot Detection System (Cell Signaling).

Small GTPase Activity Assays

To measure the activity of Rac1, Cdc42, and RhoA, pull-down assays were performed (Cell Biolabs, Inc., Rockford, IL).

Briefly, cell lysates were incubated with 2 μg of glutathione S-transferase—tagged Rho binding domain (for RhoA) and glutathione S-transferase-tagged—p21-activated kinase 1 (for Rac1 and Cdc42) at 4°C with gentle mixing. After 1 hour, the lysates were immunoblotted with antibodies specific for RhoA, Rac1, and Cdc42, as appropriate.

Cell Isolation and Culturing

Primary chondrocytes were isolated from mouse mandibular condyles according to a previously published method.[23,24] Briefly, TMJ condylar cartilage tissues were dissected from 6- to 8-week-old mice and were washed in α-minimal essential medium (MEM; Gibco, Grand Island, NY). Pieces of cartilage were minced with a scalpel and then were digested with 3 mg/mL collagenase (Wako Pure Chemical, Osaka, Japan) and 4 mg/mL dispase (Gibco) in 1× PBS at 37°C with shaking. After 3 hours, enzymatic digestion was stopped by adding α-MEM that contained 10% lot-elected fetal bovine serum (FBS; Japan Bioserum Co. Ltd., Fukuyama, Japan). The resulting cell suspension was filtered through a nylon mesh (70-μm pore size; BD Falcon, Franklin Lakes, NJ) to eliminate cell-matrix residues, then was centrifuged for 10 minutes at $250 \times g$. The chondrocytes obtained were washed 3× with α-MEM and were cultured in 5% CO_2 at 37°C in basal medium that consisted of α-MEM supplemented with 20% FBS, 2 mmol/L glutamine, 100 U/mL penicillin, 100 mg/mL streptomycin (Gibco), and 100 mmol/L 2-mercaptoethanol (Gibco). After 4 to 6 days, the adherent cells were detached with trypsin-EDTA (Gibco) and were passaged.

A mouse chondroprogenitor cell line, ATDC5 (RIKEN BioResource Center Cell Bank, Tsukuba, Japan), was cultured as a monolayer in high-glucose Dulbecco's modified Eagle's medium (Sigma-Aldrich) with 5% FBS.

Both mouse primary chondrocytes and ATDC5 cells were treated with 5 ng/mL TGF-β1 (Roche Diagnostics, Mannheim, Germany) or 10 μmol/L S1P (Cayman Chemical) when the cells reached confluence if needed.

siRNA Targeting of Smad3, S1PR3, and TGFBR2

For siRNA targeting of Smad3, a siTrio Full Set (B-Bridge International, Sunnyvale, CA) was used. Briefly, a cocktail that included three sets of sense and antisense RNA oligonucleotides: 5′-GAGGAGAAGUGGUGCGAGATT-3′ (sense) and 5′-UCUCGCACCACUUCUCCUCTT-3′ (antisense), 5′-GC-AGAGUACAGGAGACAGATT-3′ (sense) and 5′-UCUGU-CUCCUGUACUCUGCTT-3′ (antisense), and 5′-GGAGA-AUGCUGUAGGAGAATT-3′ (sense) and 5′-UUCUCCUA-CAGCAUUCUCCTT-3′ (antisense), were transfected into cells with Lipofectamine RNAiMAX (Invitrogen, Carlsbad, CA). For S1PR3-targeting siRNA, the following oligonucleotides were chemically synthesized: 5′-ACACCUAAGAG-CCAAAUUAUGCGAT-3′, 5′-GGCAUUUACGUAGGCA-CAGGGCATC-3′, and 5′-AGGAGUCACCAACGCAUUU-

CAGCCT-3′ (OriGene Technologies Inc., Rockville, MD). For siRNA that targeted TGFBR2, a siTrio Full Set (BiONEER, Daejeon, Republic of Korea) was used which included the following three sets of sense and antisense RNA oligonucleotides: 5′-GUCUACAAGGCCAAGCUGA-3′ (sense) and 5′-UCAGCUUGGCCUUGUAGAC-3′ (antisense), 5′-CAGAAGAUGGCUCGCUGAA-3′ (sense) and 5′-UU-CAGCGAGCCAUCUUCUG-3′ (antisense), and 5′-CA-CAGUGACCACACUCCUU-3′ (sense) and 5′-AAGGA-GUGUGGUCACUGUG-3′ (antisense).

Cell Transfections

Cells were plated in six-well dishes (6×10^4 cells per well). After 24 hours, the cells were transfected with Lipofectamine RNAiMAX according to the manufacturer's instructions (Life Technologies). Briefly, Lipofectamine RNAiMAX was incubated with the siRNAs in Dulbecco's modified Eagle's medium without serum and antibiotics at room temperature. After 20 minutes, the lipid/RNA complexes were added to the ATDC5 cells or the mouse primary chondrocytes isolated from mandibular condylar cartilage with gentle agitation at a final concentration of 50 nmol/L in serum that contained 1 mg/mL bovine serum albumin. The transfected cells were used for experiments within 48 hours of being transfected. Gene knockdown was confirmed by real-time PCR or Western blot analysis.

Wound Healing Assays

ATDC5 cells or mouse primary chondrocytes were plated at a high density in 12-well plates and were grown to confluence. With the use of a sterile P-200 micropipette, a scratch was made through each cell monolayer. The cells were then washed three times with PBS and were incubated in growth media with or without TGF-β. Images of the same field-of-view were obtained with a light microscope (KEYENCE) at the beginning and at the end of the experiments after each PBS wash. At least four fields were photographed for each condition at each time point, and gap distances were calculated with ImageJ software version 1.49 (NIH, Bethesda, MD; *http://imagej.nih.gov/ij*). Wound healing was defined as a reduction in the gap distance over time.

Cell Migration Assays

To evaluate the chemotaxis stimulated by S1P and TGF-β in primary mandibular chondrocyte cell cultures derived from WT and $Smad3^{-/-}$ mice, a Cultrex 96-well Cell Migration Assay kit (Trevigen, Gaithersburg, MD) was used according to the manufacturer's instructions. Before the assay, cells were starved for 24 hours in serum-free medium and then were incubated in Dulbecco's modified Eagle's medium without FBS in the presence of S1P and TGF-β for 8 hours. The cells were also pretreated with inhibitors, including FTY720 (BioVision, San Francisco, CA) and suramin (Sigma-Aldrich) for 1 hour before the migration assays were performed.
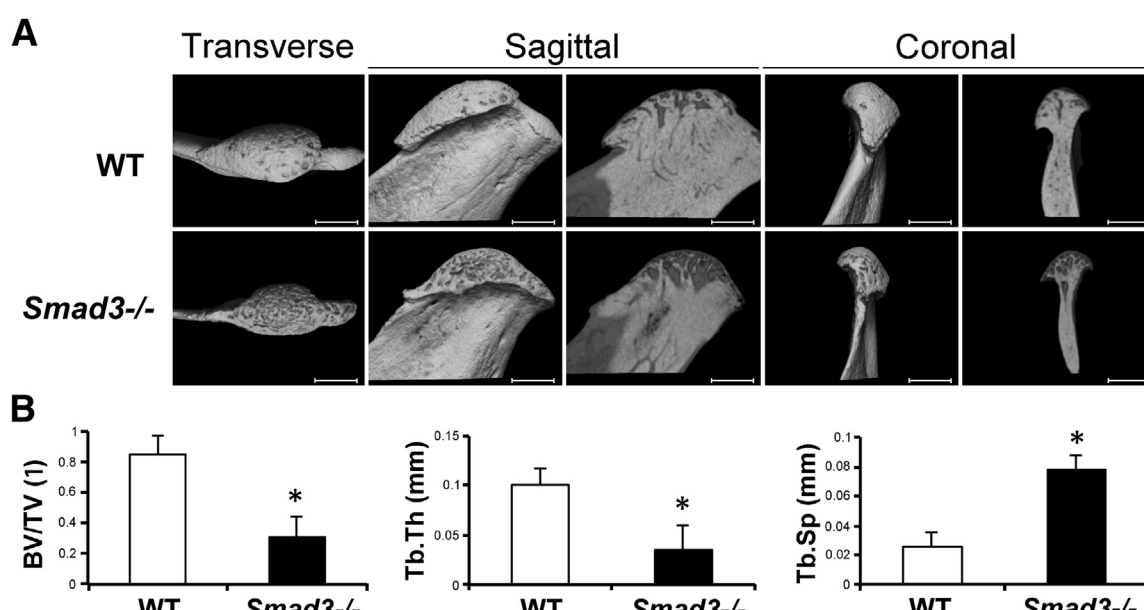
Figure 1 The effect of *Smad3* deficiency on mandibular condyles. **A:** A three-dimensional reconstruction of mandibular condyles from 4-month-old *Smad3*$^{-/-}$ and WT mice. Representative transverse, sagittal, and coronal views from micro-CT scans of the condyles. **B:** Trabecular BV was determined in representative sagittal plane sections, and these values are presented as BV/TV ratio. Data are expressed as means $\pm$ SD. $n = 5$. *$P < 0.05$. Scale bar = 500 μm. BV, bone volume; micro-CT, microcomputed tomography; Tb.Sp, trabecular separation; Tb.Th, trabecular thickness. TV, tissue volume; WT, wild-type.

3D Matrigel Cultures

To evaluate the influence of extracellular matrix (ECM) components, 3D Matrigel cultures were grown in six-well plates. Growth factor-reduced Matrigel (Trevigen) was handled according to the manufacturer's instructions. ATDC5 cells transfected with *Smad3*-targeted siRNA or primary chondrocyte cells transfected with *S1PR3*-targeted siRNA with the use of 3D-Fectin transfection reagent (OZ Biosciences, Marseille, France) were cultured on this Matrigel and were incubated in the presence of 5 ng/mL TGF-β1 for 0 to 30 minutes. Cell lysates were subsequently isolated with a 3D Culture Cell Harvesting Kit (Trevigen).

Statistical Analysis

All experiments were performed at least in triplicate for each set of conditions, and each experiment was independently repeated at least two or three times. The results are presented as the means $\pm$ SD. These data were statistically analyzed with *t*-test or one-way analysis of variance with post hoc Tukey honest significant differences test, as appropriate for each case. $P < 0.05$ was considered statistically significant.

Results

Maintenance of Normal Condylar Cartilage and a Role for Smad3

To evaluate the role of Smad3 in mandibular condyle development and maintenance, the TMJs of *Smad3*$^{-/-}$ mice were analyzed. The micro-CT results found that the bone volume-to-trabecular volume ratio and the trabecular thickness were reduced among different regions of the condylar subchondral bone in the 4-month-old *Smad3*$^{-/-}$ mice compared with the age-matched WT mice (Figure 1, A and B). In contrast, the trabecular separation was significantly greater in the 4-month-old *Smad3*$^{-/-}$ mice than in the age-matched WT mice (Figure 1, A and B), thereby indicating the dynamic nature of bone mineral density and microstructure in *Smad3*$^{-/-}$ mice. The phenotype of the *Smad3*$^{-/-}$ mice was also more prominent in the mandibular condylar cartilage. For example, Smad3-dependent differences were apparent in the 4-month-old mice on the basis of the decrease in overall safranin O staining with fast green and the reduced toluidine blue staining in each TMJ that were observed. These observations also became more prominent with age (Figure 2, D–F). The modified Mankin scores that were assigned[22] further confirmed that deficiency of Smad3 caused important changes in structural characteristics that parallel the progression of OA (Figure 2G). Other hallmarks of OA were observed in the condylar cartilage of the 4-month-old *Smad3*$^{-/-}$ mice, including deterioration of the smooth articular cartilage surface and fibrillation of the superficial layer (Figure 2, A and D). Consistent with previous *in vitro* studies of osteoclastogenesis in bone marrow cells of *Smad3*$^{-/-}$ mice,[25] few osteoclasts were present in the condylar subchondral bone of the *Smad3*$^{-/-}$ mice examined (Figure 2, B and C).

Smad3 Maintains a Normal Cartilage Matrix Composition

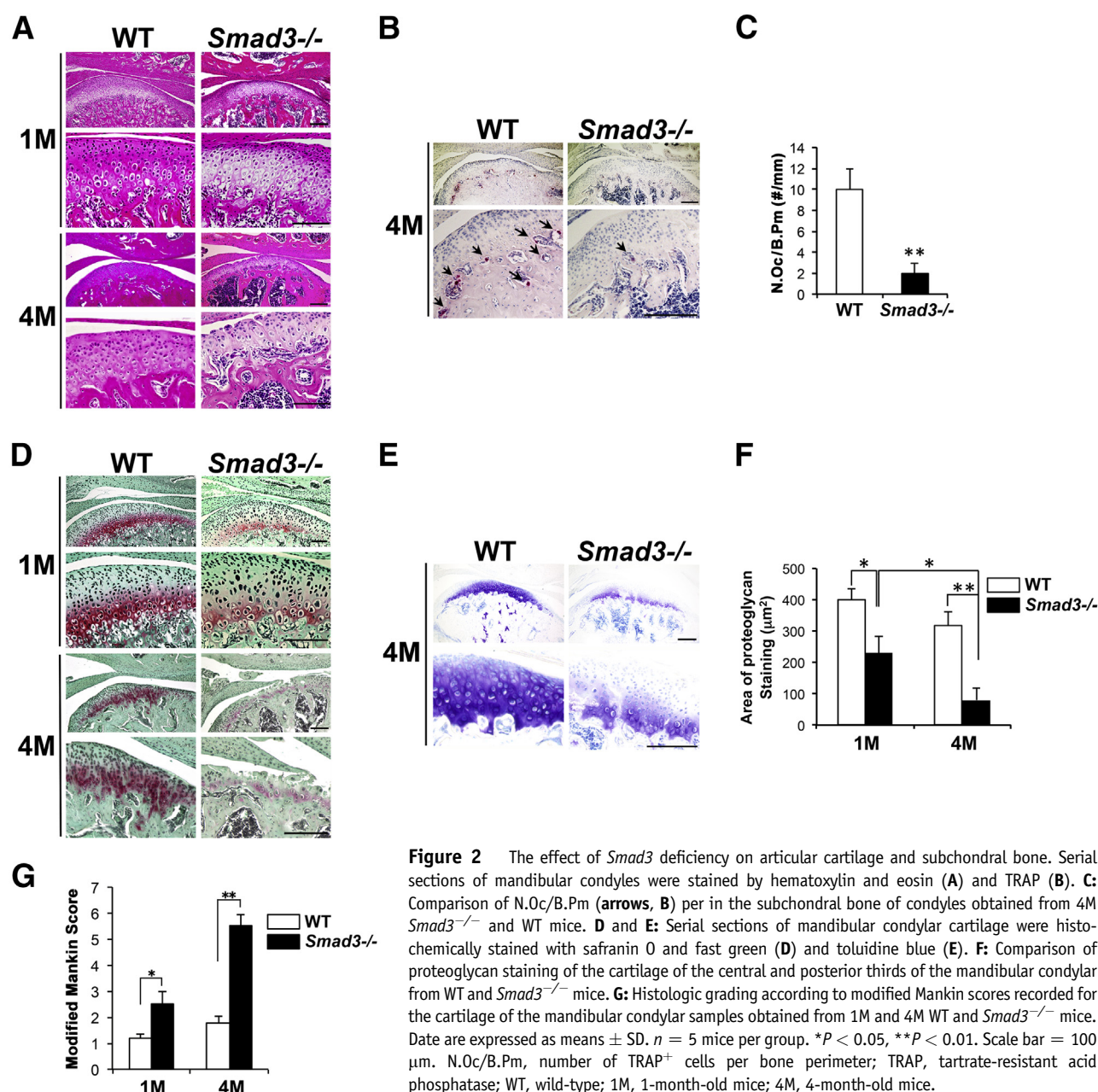To investigate the molecular basis of the Smad3-dependent differences observed in the structure and

[F1]

[F2]

Figure 2 The effect of *Smad3* deficiency on articular cartilage and subchondral bone. Serial sections of mandibular condyles were stained by hematoxylin and eosin (**A**) and TRAP (**B**). **C:** Comparison of N.Oc/B.Pm (**arrows**, **B**) per in the subchondral bone of condyles obtained from 4M *Smad3*$^{-/-}$ and WT mice. **D** and **E:** Serial sections of mandibular condylar cartilage were histochemically stained with safranin O and fast green (**D**) and toluidine blue (**E**). **F:** Comparison of proteoglycan staining of the cartilage of the central and posterior thirds of the mandibular condylar from WT and *Smad3*$^{-/-}$ mice. **G:** Histologic grading according to modified Mankin scores recorded for the cartilage of the mandibular condylar samples obtained from 1M and 4M WT and *Smad3*$^{-/-}$ mice. Date are expressed as means ± SD. $n = 5$ mice per group. *$P < 0.05$, **$P < 0.01$. Scale bar = 100 μm. N.Oc.B.Pm, number of TRAP$^+$ cells per bone perimeter; TRAP, tartrate-resistant acid phosphatase; WT, wild-type; 1M, 1-month-old mice; 4M, 4-month-old mice.

composition of the cartilage matrix, mRNA levels of Col2a1 and aggrecan were detected. The corresponding proteins represent key components of the cartilage matrix. Levels of Col2a1 mRNA were reduced by 50% in the cartilage samples obtained from 4-month-old *Smad3*$^{-/-}$ mice compared with the cartilage samples obtained from age-matched, control littermates (Figure 3A). Progressive loss of the Col2a1 and aggrecan proteins and loss of Smad3 phosphorylation were also observed in Western blot analysis and immunohistochemistry assay of the articular cartilage of the *Smad3*$^{-/-}$ mice (Figure 3, B and C, and Supplemental Figure S1A). Taken together, these results suggest that

Smad3 is essential for the sustained expression of two key components of the cartilage matrix, Col2a1 and aggrecan.

Levels of MMP-13 and MMP-9 Are Higher in Condylar Cartilage Obtained from *Smad3*$^{-/-}$ Mice

Degenerative changes in the cartilage matrix may result from reduced matrix synthesis, increased matrix degradation, or both. To distinguish these possibilities, expression levels and localization of MMPs, MMP-13 and MMP-9, were examined. MMP-13 and MMP-9 degrade aggrecan and Col2a1, respectively, and are present at higher levels during OA.
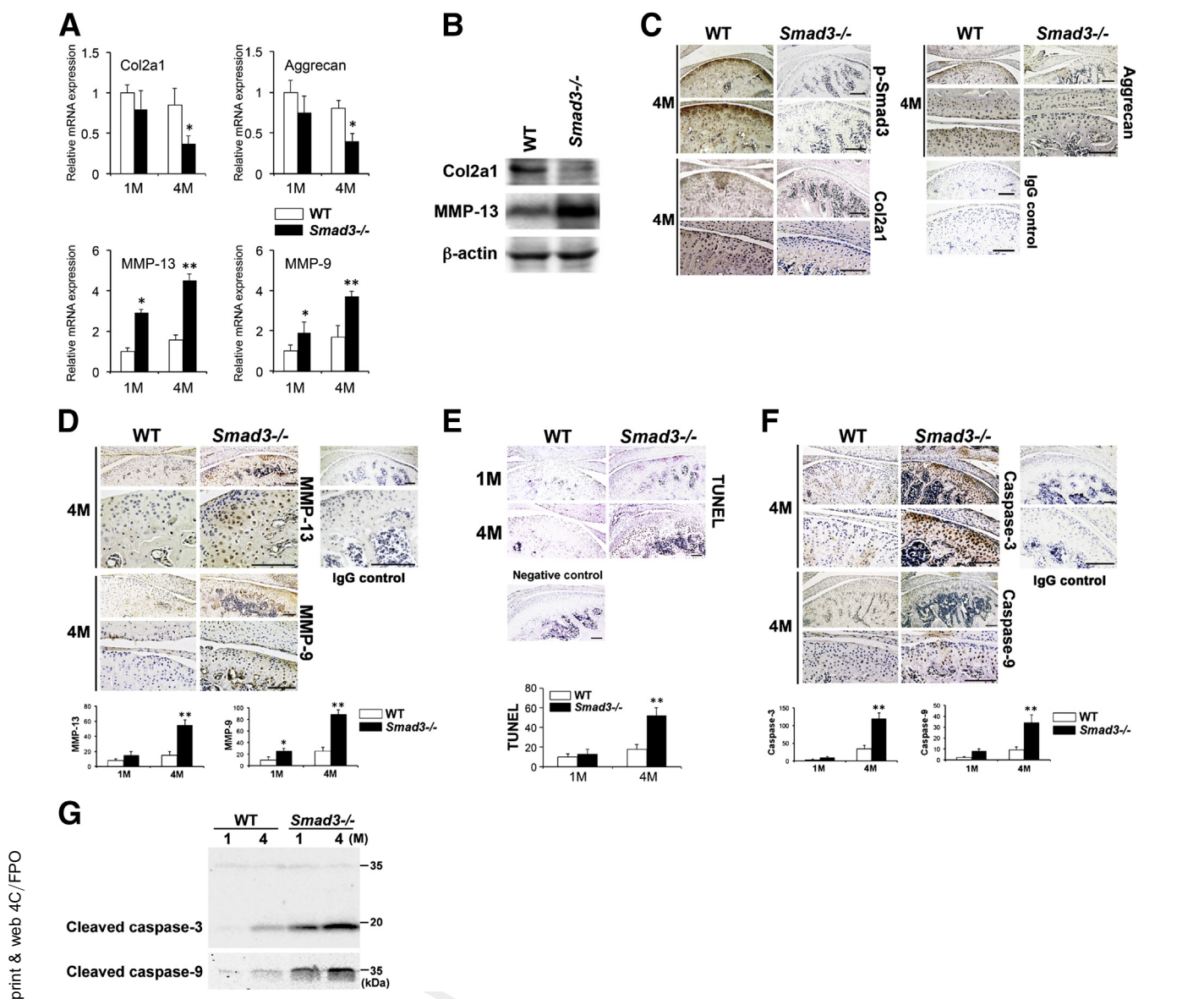
Figure 3 Molecular composition of the mandibular condylar cartilage in *Smad3*$^{-/-}$ mice. **A:** mRNA levels of Col2a1, aggrecan, MMP-13, and MMP-9 were detected in mandibular condylar cartilage samples obtained from 1M and 4M *Smad3*$^{-/-}$ mice and their littermates. Expression of each mRNA was quantified and normalized to GAPDH. The real-time PCR results are representative of independent experiments. **B:** Western blot analysis of Col2a1 and MMP-13 expression in mandibular condylar cartilage obtained from WT and *Smad3*$^{-/-}$ littermates. β-Actin was used as an internal control. **C:** Immunohistochemical analysis of phosphorylated Smad3, Col2a1, and aggrecan in mandibular articular cartilage samples obtained from 4M WT and *Smad3*$^{-/-}$ littermates. As a negative control, mandibular articular cartilage obtained from 4M WT mice were stained with rabbit IgG (isotype control). **D:** The distribution of MMP-13 and MMP-9 proteins in 4M *Smad3*$^{-/-}$ articular cartilage. As a negative control, mandibular articular cartilage obtained from 4M *Smad3*$^{-/-}$ mice were stained with rabbit IgG (isotype control). The number of MMP-13$^+$ and MMP-9$^+$ cells in the central and posterior thirds of the mandibular condylar cartilage samples from WT and *Smad3*$^{-/-}$ mice were examined. **E:** Serial sections of condylar cartilage obtained from 1M and 4M *Smad3*$^{-/-}$ mice were stained in TUNEL assays. As a negative control, mandibular articular cartilage obtained from 4M *Smad3*$^{-/-}$ mice were stained with TdT substrate solution without TdT. The number of TUNEL$^+$ cells in the central and posterior thirds of the mandibular condylar cartilage obtained from WT and *Smad3*$^{-/-}$ mice were compared. **F:** Serial sections of condylar cartilage from 4M *Smad3*$^{-/-}$ mice were immunostained for active caspase-3 and caspase-9. As a negative control, mandibular articular cartilage obtained from 4M *Smad3*$^{-/-}$ mice were stained with rabbit IgG (isotype control). The number of active caspase-3$^+$ and caspase-9$^+$ cells in the central and posterior thirds of the mandibular condylar cartilage obtained from WT and *Smad3*$^{-/-}$ mice were compared. **G:** Immunoblot analysis of cleaved caspase-3 and cleaved caspase-9 in primary mandibular chondrocyte cells isolated from 1M and 4M WT and *Smad3*$^{-/-}$ mice. Data are expressed as means ± SD. $n = 5$ mice per group (**A**); $n = 3$ independent experiments (**A** and **B**); $n = 2$ independent experiments (**G**). *$P < 0.05$, **$P < 0.01$. Scale bar = 100 μm. Col2a1, type II collagen; GAPDH, glyceraldehyde 3-phosphate dehydrogenase; MMP, matrix metallopeptidase; TUNEL, TdT-mediated dUTP-digoxigenin nick-end labeling; 1M, 1-month-old mice; 4M, 4-month-old mice.

Unlike their control littermates, the mRNA levels of MMP-13 and MMP-9 that were detected in the articular cartilage samples obtained from *Smad3*$^{-/-}$ mice were highly variable (Figure 3A). Moreover, an increased distribution of MMP-13 and MMP-9 proteins was consistently observed in both the proliferative and hypertrophic layers of the cartilage samples obtained from the 4-month-old *Smad3*$^{-/-}$ mice (Figure 3D and Supplemental Figure S1B).

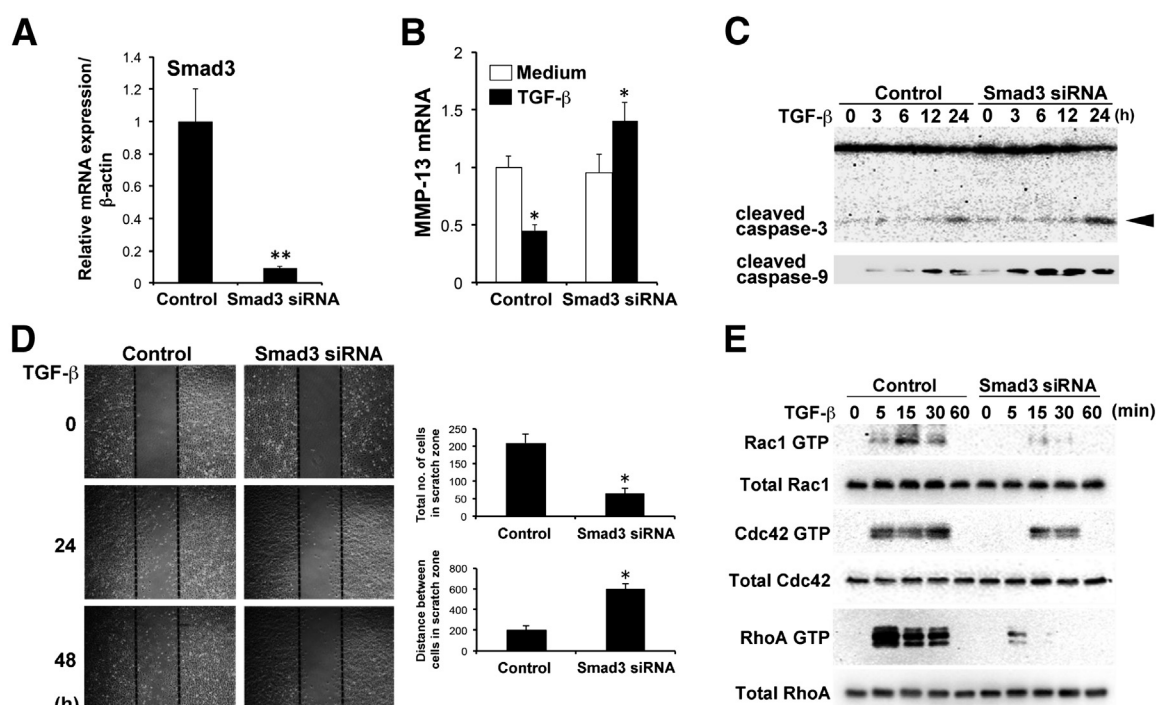FLA 5.4.0 DTD ■ AJPA2116_proof ■ 20 August 2015 ■ 2:19 pm ■ EO: AJP14_0737

Figure 4 Effect of *Smad3*-targeted siRNA on chondrocyte functions. **A:** Relative mRNA levels of Smad3 in mouse chondroprogenitor ATDC5 cells were detected by real-time PCR 48 hours after transfection with control siRNA and *Smad3*-targeted siRNA. **B:** ATDC5 cells were transfected with *Smad3*-targeting siRNA and were incubated in the presence or absence of 5 ng/mL TGF-β1 for 8 hours. Messenger RNA levels of MMP-13 were detected by real-time PCR. **C:** ATDC5 cells were transfected with *Smad3*-targeted siRNA and were incubated in the presence or absence of 5 ng/mL TGF-β1 for 0, 3, 6, 12, and 24 hours. Total cell lysates (50 μg) were subjected to Western blot analysis to detect cleaved caspase-3 and cleaved caspase-9. **D:** ATDC5 cells were prepared as described in **A** and were evaluated in wound healing assays. Cell migration is quantified in the **lower panel. E:** ATDC5 cells were transfected with *Smad3*-targeted siRNA and were incubated in the presence or absence of 5 ng/mL TGF-β1 for 0 to 60 minutes. Total cell lysates (50 μg) were subjected to Western blot analysis to detect expression of Rac1-GTP, Cdc42-GTP, and RhoA-GTP. Data are expressed as means ± SD. *n* = 3 independent experiments that displayed similar results (**A**); *n* = 2 independent experiments (**C** and **E**); *n* = 4 of three independent experiments. *$P < 0.05$, **$P < 0.01$. MMP, matrix metallopeptidase; TGF, transforming growth factor.

Higher Numbers of Apoptotic Chondrocytes Are Present in the *Smad3*$^{-/-}$ Mice

Studies have suggested that cell death in OA cartilage occurs primarily via apoptosis.[26,27] The cartilage obtained from the 4-month-old *Smad3*$^{-/-}$ mice exhibited a greater number of cell-free regions, and these were accompanied by extensive areas of proteoglycan loss (Figure 2, A and D−G). TUNEL assays were subsequently performed to determine whether abnormal chondrocyte apoptosis preferentially occurred in degraded cartilage. In WT mice, the number of TUNEL$^+$ chondrocytes was low. However, in the mildly degraded areas of cartilage obtained from the 4-month-old *Smad3*$^{-/-}$ mice, a marked increase in the number of TUNEL$^+$ cells was observed, and these cells were predominantly located in the proliferative and hypertrophic layers of the cartilage (Figure 3E).

In the present study, detection of cleaved caspase-3 and cleaved caspase-9 represented a means by which to distinguish apoptotic chondrocytes from cells that died by other mechanisms, such as necrosis.[26,28] In the mandibular condylar cartilage obtained from the *Smad3*$^{-/-}$ mice, cells positive for cleaved caspase-3 and caspase-9 were progressively distributed within whole layers of the cartilage (Figure 3F and Supplemental Figure S1C). In contrast, low levels of cleaved caspase-3 and cleaved caspase-9 were detected in the condylar cartilage tissues of WT mice. Moreover, these expression levels were confirmed by Western blot analysis (Figure 3G). Taken together, these results strongly suggest that TGF-β/Smad3 signaling contributes to the apoptosis of mandibular condylar cartilage cells via activated caspase signaling cascades.

Effects of *Smad3*-Targeted siRNA on Chondroprogenitor Cell Functions

To more precisely examine the effects of TGF-β and Smad3 on the functions of chondrocytes, and to confirm the molecular mechanisms that mediate breakdown of the mandibular condylar cartilage in *Smad3*$^{-/-}$ mice, the mouse embryonal carcinoma-derived cell line ATDC5 was used as a model of chondroprogenitor cells. First, ATDC5 cells were transfected with *Smad3*-targeted siRNA. A 95% reduction in Smad3 mRNA levels was achieved relative to the levels detected in cells transfected with control siRNA (Figure 4A). On the basis of the results described above whereby increased expression of MMP-13 corresponded [F4]

with increased proteolysis of Col2a1 and aggrecan and progressive degradation of mandibular condyle cartilage (Figure 3, A–D, and Supplemental Figure S1, A and B), MMP-13 expression was also assayed in ATDC5 cells. In the ATDC5 cells that expressed the control siRNA, TGF-β–mediated repression of MMP-13 mRNA was detected. In contrast, TGF-β–mediated repression of MMP-13 mRNA was absent in cells that expressed the *Smad3*-targeted siRNAs (Figure 4B). To confirm the enhanced apoptotic signaling that was detected in the mandibular condylar cartilage of the *Smad3*$^{-/-}$ mice (Figure 3, E–G, and Supplemental Figure S1C), cleavage of caspase-3 was assayed after the transfection of *Smad3*-targeting siRNA. The active form of caspase-3 was found to be markedly up-regulated 24 hours after TGF-β stimulation, whereas only a slight increase in levels of cleaved caspase-3 were detected in ATDC5 cells transfected with the control siRNA. Similarly levels of cleaved caspase-9 in ATDC5 cells transfected with *Smad3*-targeted siRNA increased between 3 and 24 hours after TGF-β stimulation, whereas only a slight increase in the levels of cleaved caspase-9 were detected in the ATDC5 cells transfected with the control siRNA (Figure 4C). These data support the *in vivo* findings that Smad3 may contribute to the maintenance of condylar cartilage via caspase signaling cascades.

Endochondral bone formation begins with the migration and condensation of chondroprogenitor cells. Subsequently, overt chondrogenesis provides a cartilaginous mold for bone formation in mammals.[29] To clarify the molecular basis of Smad3 participation in the regulation of chondrocyte migration, ATDC5 cells were subjected to a wound healing/scratch assay. The ATDC5 cells that were transfected with the *Smad3*-targeted siRNA found a greater decrease in cell motility in response to TGF-β than the ATDC5 cells transfected with the control siRNA (Figure 4D). Moreover, when the activity of Rac1-GTP, Cdc42-GTP, and RhoA-GTP were assayed, time-dependent increases in the corresponding activity levels were detected after TGF-β stimulation in the ATDC5 cells transfected with the control siRNA. In contrast, the activity levels of these three Rho GTPases in the ATDC5 cells transfected with *Smad3*-targeted siRNA were repressed after TGF-β stimulation (Figure 4E). These experiments were also performed on a 3D gel matrix that was shown to optimally activate migration-organizing molecules in response to TGF-β (Supplemental Figure S2A). Similarly, the activities of these three Rho GTPases in the ATDC5 cells transfected with *Smad3*-targeted siRNA were repressed after TGF-β stimulation (Supplemental Figure S2B).

Expression of Sphk1 and S1P$_3$ Reduces in Smad3-Deficient Chondrocytes

The S1P receptor is expressed on the cell surface and is internalized on binding of an S1P ligand as part of the migratory response.[30] To analyze the expression of the S1P receptor, primary mandibular chondrocytes were isolated.

These cells were found to express high levels of Sox9 and Col2a1 mRNA, they were positive for Alcian Blue staining, and they were positive for Col2a1 expression by immunocytochemistry (Supplemental Figure S3, A and B). Col2a1 is a marker of the chondrogenic lineage. With the use of real-time PCR, mRNA levels of Sphk1 and S1P$_{1-5}$ were also detected in the primary mandibular chondrocyte cells isolated from WT and *Smad3*$^{-/-}$ mice. No differences were found in the mRNA levels of S1P$_1$, S1P$_2$, S1P$_4$, and S1P$_5$ that were detected between the two sets of samples. However, significantly lower levels of Sphk1 and S1P$_3$ mRNAs were detected in the *Smad3*$^{-/-}$ chondrocytes than in the WT chondrocytes (Figure 5A). When the same cells were [F5] analyzed by Western blot analysis for expression of Sphk1, S1P$_1$, and S1P$_3$, protein levels of Sphk1 and S1P$_3$ were found to be significantly lower in the *Smad3*$^{-/-}$ chondrocyte extracts than in the WT chondrocyte extracts (Figure 5B). In contrast, the levels of S1P$_1$ remained largely unchanged. When expression levels of Sphk1, S1P$_1$, and S1P$_3$ were detected in the mandibular condyles of WT and *Smad3*$^{-/-}$ mice by immunohistochemical analysis, Sphk1 and S1P$_3$ expression levels were significantly lower in the latter than in the former (Figure 5C).

It was reported that Sox9 and Col10a1 are cartilage-specific genes.[31–33] In addition, OA chondrocytes were found to express lower levels of Sox9; overexpression of Sox9 was found to restore the ECM of OA tissue.[34] When OA chondrocytes from the *Smad3*$^{-/-}$ and WT mice were analyzed by real-time PCR and Western blot analysis, mRNA and protein levels of Sox9 were found to be significantly lower in the *Smad3*$^{-/-}$ chondrocyte extracts than in the WT chondrocyte extracts. Accumulating evidence suggests that the expression of Col10a1 is elevated in human OA cartilage as a result of chondrocyte hypertrophy and cartilage calcification.[35,36] Up-regulation of Col10a1 was also reported in experimental OA animal models.[37] Expression levels of Col10a1 in the *Smad3*$^{-/-}$ chondrocyte extracts were significantly higher than the levels detected in the WT chondrocyte extracts (Supplemental Figure S3, C and D). Similarly, expression levels of Col10a1 were significantly higher in the condylar cartilage samples obtained from *Smad3*$^{-/-}$ mice than the expression levels detected in the WT mice by immunohistochemical analysis (Supplemental Figure S3E).

Quantitative analysis of S1P receptor expression was also performed with real-time PCR, and it was confirmed that TGF-β1 strongly affected levels of S1P receptor mRNA in primary chondrocytes derived from WT mice. In particular, a marked increase in S1P$_3$ and Sphk1 mRNA levels were detected in primary chondrocytes derived from WT mice that were treated for 24 hours with TGF-β. In contrast, the same TGF-β treatment of primary chondrocytes derived from *Smad3*$^{-/-}$ mice did not induce an increase in S1P$_3$ and Sphk1 mRNA levels (Figure 5D).

Next, cell migration in relation to TGF-β/Smad3 and S1P/S1P receptor signaling was investigated with an S1P

receptor agonist, FTY720, and an S1P$_3$ antagonist, suramin. WT chondrocytes migrated in response to stimulation by TGF-β and S1P, whereas migration was inhibited after pretreatment with FTY720 or suramin (Figure 5E). Taken together, these data indicate that crosstalk occurs between the TGF-β/Smad3 and S1P/S1P$_3$ signaling pathways in mandibular condylar chondrocytes.
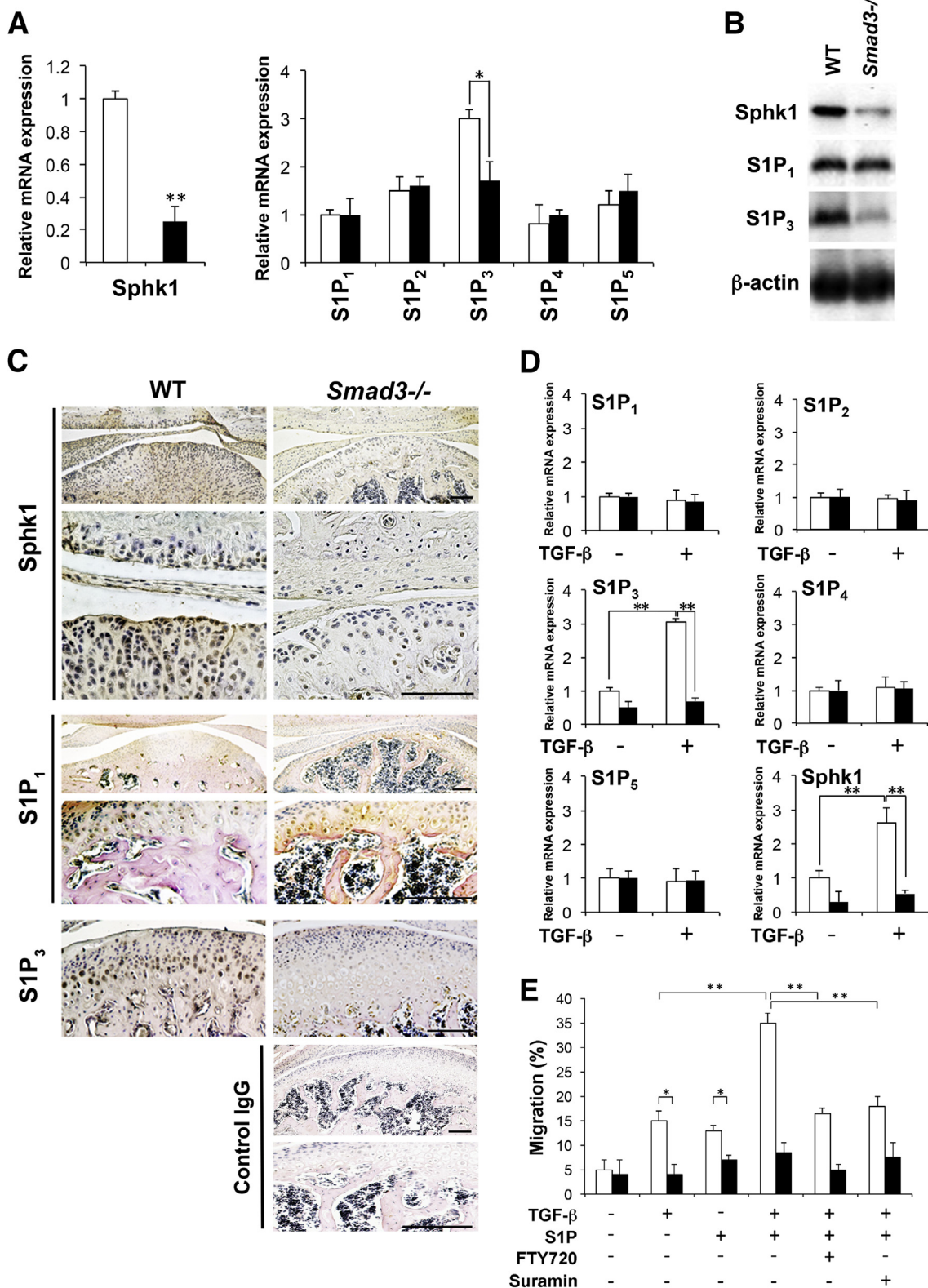
Crosstalk between TGF-β/Smad3 and S1P/S1P₃ Signaling Pathways Regulates the Migratory Function of Chondrocytes

To examine whether S1P₃ regulates chondrocyte migration, primary chondrocytes were isolated from the mandibular condylar cartilage of WT mice and were transfected with S1P₃-targeted siRNA. A 75% reduction in mRNA and protein levels of S1P₃ was achieved relative to the cells transfected with the control siRNA (Figure 6, A and B). When both sets of transfected cells were treated with S1P for various periods of time, S1P-stimulated phosphorylation of Smad3 was found to be inhibited in the cells transfected with S1P₃-targeted siRNA compared with the cells transfected with the control siRNA (Figure 6C).

It was reported that stimulation of mesangial cells with S1P leads to rapid activation of all three major mitogen-activated protein kinase signaling cascades, ERK, p38, and c-Jun N-terminal kinase.[38] Activation of these cascades can be detected by measuring the phosphorylation levels of different members of these cascades. Phosphorylation of Akt and the mitogen-activated protein kinase signaling targets, ERK and p38, rapidly increased in the primary chondrocytes that were transfected with the control siRNA and then stimulated with S1P (Figure 6C). In contrast, decreased phosphorylation of Akt, ERK, and p38 was detected in the primary chondrocytes that were transfected with the S1P₃-targeted siRNA and then stimulated with S1P (Figure 6C). When the primary chondrocytes were pretreated with the S1P₃ antagonist, suramin, 1 hour before stimulation with S1P for 15 minutes, S1P-stimulated Smad3 phosphorylation was inhibited (Figure 6D). These results suggest that S1P transactivates Smad3 in an S1P₃-dependent manner.

Finally, the involvement of TGF-βR II in S1P signaling was investigated after the transfection of TGFBR2-targeting siRNA. The down-regulation of TGF-βR II abrogated S1P-induced Smad3 phosphorylation (Figure 6E). In addition, Western blot analysis of the same cell lysates confirmed that lower levels of TGF-βR II protein were present after the transfection of TGFBR2-targeting siRNA versus the control RNA (Figure 6E).

In a wound healing/scratch assay, primary chondrocytes that were isolated from mandibular condylar tissue and transfected with a S1PR3-targeting siRNA exhibited a greater decrease in cell motility in response to TGF-β than the control cells (Figure 6F). Small GTPase activity levels for key downstream targets of G protein-signaling cascades were also assayed, and these included Rac1-GTP, RhoA-GTP, and Cdc42-GTP. The activity levels of these signal transduction proteins were enhanced in the cells transfected with the control siRNA and were not enhanced in the chondrocytes that were transfected with S1PR3-targeting siRNA and then stimulated with TGF-β (Figure 6G). When the primary chondrocytes were grown in a 3D gel matrix after being transfected with S1PR3-targeted siRNA, the activity of these three Rho GTPases were repressed after TGF-β stimulation (Supplemental Figure S2C).

Discussion

Here, bone mineral density, subchondral bone volume, and osteoclast activities were reduced in the mandibular condyles of the Smad3⁻/⁻ mice examined. In addition, the articular surfaces were collapsed, the thickness of the articular cartilage was reduced, and the abundance of cartilage matrix proteins was progressively decreased. As a result, erosion of the articular cartilage of the mandibular condyles had occurred. Previously, Smad3⁻/⁻ mice were characterized by a diminished T-cell response to TGF-β,[20,39] accelerated wound healing,[40] and a higher incidence of colon cancer.[41]

TGF-β1–induced Smad activation was shown to inhibit the expression of proteases that regulate degradation of the ECM (eg, MMPs) and to inhibit the proteolysis of cell surface membrane proteins during physiologic processes. The latter include embryonic development and wound healing, whereas the affected pathologic conditions include cancer and tissue fibrosis.[42] Here, degradation of the Smad3⁻/⁻ mandibular condylar cartilage was associated with impaired anabolic activity and increased cartilage degradation. MMP-13 and MMP-9 were shown to contribute to the breakdown of articular cartilage and the resorption of subchondral bone,[43–45] and both are important contributors to the histologic phenotype of OA. Smad3⁻/⁻ mandibular chondrocytes were found to express higher

Figure 5 Expression of S1P receptors by chondrocytes from Smad3⁻/⁻ mice. **A:** Mandibular primary chondrocyte cells were isolated from WT (white bars) and Smad3⁻/⁻ (black bars) mice and were subjected to real-time PCR analysis with the use of primers specific for Sphk1, S1P₁, S1P₂, S1P₃, S1P₄, S1P₅, and GAPDH. **B:** Immunoblot analysis of mandibular primary chondrocyte cells isolated from 4-month-old WT and Smad3⁻/⁻ littermates. Reduced expression of Sphk1 and S1P₃ were detected in the articular cartilage. Detection of β-actin was used as an internal control. **C:** Immunohistochemical analysis of mandibular articular cartilage obtained from 4-month-old WT and Smad3⁻/⁻ mice. Reduced expression of Sphk1 and S1P₃ were detected in the articular cartilage. As a negative control, mandibular articular cartilage obtained from 4-month-old Smad3⁻/⁻ mice were stained with rabbit IgG (isotype control). **D:** A quantitative analysis of Sphk1 and S1P₁₋₅ mRNA levels detected by real-time PCR with the use of total RNA extracted from mandibular primary chondrocyte cells obtained from 4-month-old WT and Smad3⁻/⁻ mice that were stimulated (+) or not (−) with 5 ng/mL TGF-β1 for 48 hours. Fold-change data, according to the $2^{-\Delta\Delta C_T}$ method (with the S1P₃ subtype used for calibration), are presented **E:** Migration assays of WT and Smad3⁻/⁻ chondrocyte cells that were pretreated for 1 hour with FTY720 or suramin and then were incubated with 5 ng/mL TGF-β or 10 μmol/L S1P. Data are expressed as means ± SD. $n = 3$ independent experiments that displayed similar results (**A**); $n = 3$ independent experiments (**B**); $n = 5$ mice from each group (**C**); $n = 1$ representative experiment performed in triplicate and repeated three times with analogous results (**D**); $n = 3$ from three independent experiments (**E**). *$P < 0.05$, **$P < 0.01$. Scale bar = 100 μm. GAPDH, glyceraldehyde 3-phosphate dehydrogenase; SIP, sphingosine 1-phosphate; S1P₁₋₅, sphingosine 1-phosphate receptor 1–5; Sphk, sphingosine kinase; TGF, transforming growth factor; WT, wild-type.
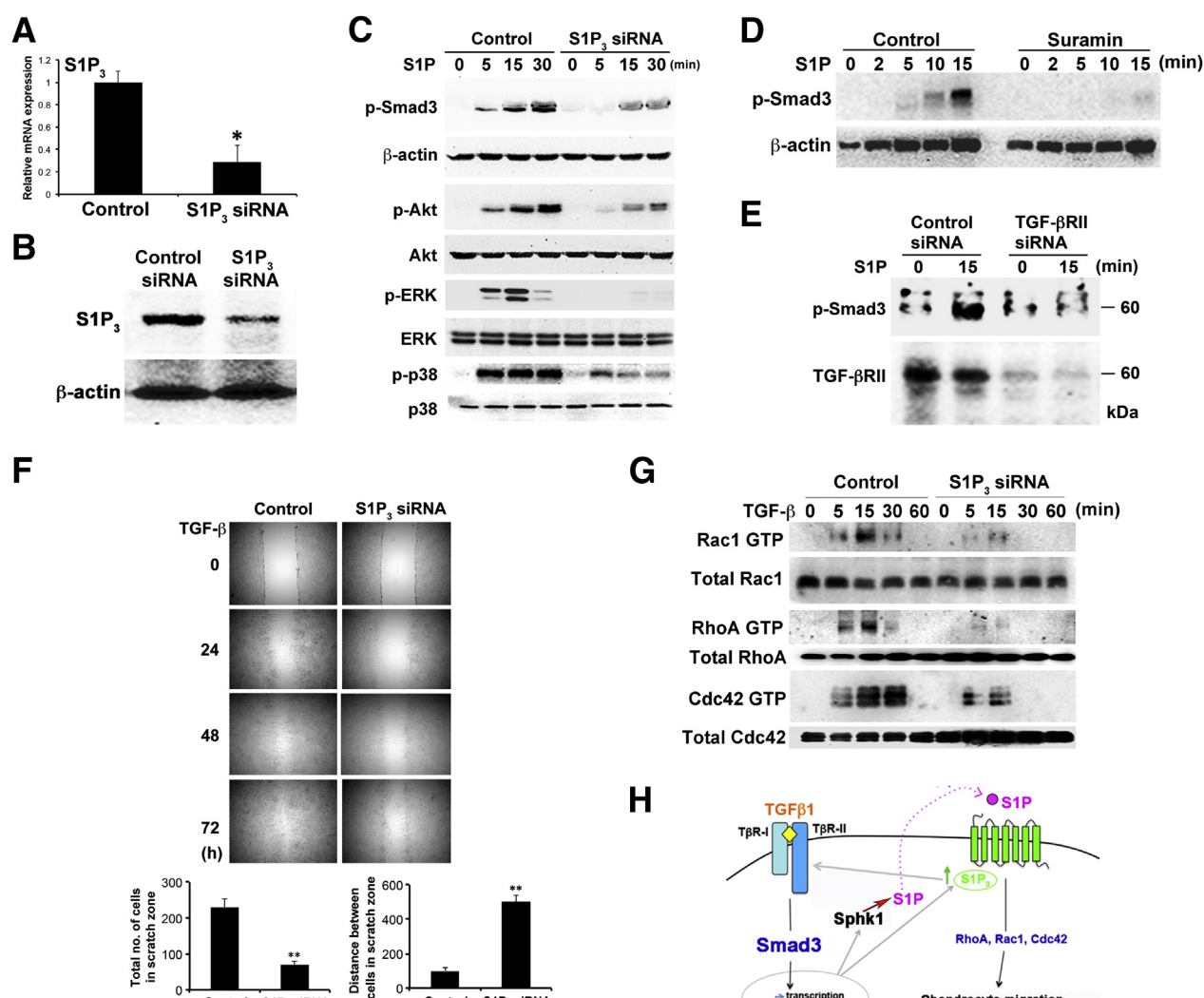
Figure 6 Effect of *S1PR3*-targeted siRNA on chondrocyte functions. **A:** Relative mRNA levels of S1P$_3$ were detected by real-time PCR in primary chondrocyte cells transfected with control and *S1PR3*-targeted siRNAs. Expression levels were normalized to GAPDH. **B:** After the transfection of primary chondrocyte cells with control and *S1PR3*-targeted siRNAs for 48 hours, S1P$_3$ protein levels were detected by Western blot analysis. Detection of β-actin was used as a loading control. **C:** Primary chondrocyte cells were transfected with control or *S1PR3*-targeted siRNAs and were subsequently stimulated with 10 μmol/L S1P for the indicated time points. Western blot analyses used primary antibodies that recognize p-Smad3, p-Akt, p-ERK, and p-p38. **D:** Primary chondrocytes were treated with suramin and then stimulated with 10 μmol/L S1P for the indicated time periods. Western blot analyses were performed with a p-Smad3 primary antibody. **E:** Primary chondrocytes were transfected with control siRNA or mouse *TGFBR2*-targeted siRNA and then were stimulated with either vehicle or 10 μmol/L S1P (15 minutes). **F:** Primary chondrocytes were transfected with control or *S1PR3*-targeted siRNAs, stimulated with 5 ng/mL TGF-β for the indicated time periods, and then subjected to wound healing assays. Cell migration is quantified in the **lower panel. G:** Primary chondrocytes were transfected with control or *S1PR3*-targeted siRNAs and then stimulated with 5 ng/mL TGF-β for the indicated time periods. The activity levels of Rac1-GTP, RhoA-GTP, and Cdc42-GTP were measured in pull-down assays. **H:** A proposed model for the mechanisms by which crosstalk between the TGF-β/Smad3 and S1P/S1P$_3$ signaling pathways regulate chondrocyte migration. Data are expressed as means ± SD. $n = 3$ for each from three independent experiments (**A**); $n = 3$ independent experiments (**B–G**). *$P < 0.05$, **$P < 0.01$. ERK, extracellular signal-regulated kinase; GAPDH, glyceraldehyde 3-phosphate dehydrogenase; p, phospho; S1P, sphingosine 1-phosphate; S1P$_3$, sphingosine 1-phosphate receptor 3; Sphk, sphingosine kinase; TGF, transforming growth factor; TGF-βRII, transforming growth factor-β type II receptor.

levels of MMP-13 and MMP-9 in the hypertrophic layer of the condylar cartilage in 4-month-old *Smad3$^{-/-}$* mice than in the same tissue in 1-month-old *Smad3$^{-/-}$* mice. In addition, the former synthesized less Col2a1 and aggrecan, both of which are substrates for MMP-13 and MMP-9. Taken together, these results are consistent with the degradation and remodeling of the mandibular condylar cartilage that were observed in the 4-month-old *Smad3$^{-/-}$* mice examined.

The results of the present study indicate that spontaneous abnormalities in the mandibular condyle subchondral bone can induce progressive cartilage degradation in mice. These results are consistent with a mouse model of chondrocyte-specific deletion of *Smad3* that has provided a model of OA in the knee joint.[46] In humans, mutations in *Smad3* were found in the MH2 domain of the Smad3 protein, a region that is extremely well conserved among other species and

among other Smad proteins that are associated with early-onset OA.[47] Moreover, it was recently reported that over-expression of TGF-β1 in subchondral bone leads to mandibular condyle degradation in mice.[48]

Chondrocyte death is commonly accepted as a hallmark of OA[28] and appears to positively correlate with the severity of matrix depletion and destruction that are observed in osteoarthritic cartilage.[28,49] In the present study, cell death in the condylar cartilage of Smad3$^{-/-}$ mice also appeared to be progressive, because the numbers of both TUNEL$^+$ and active caspase-3$^+$ and caspase-9$^+$ cells were not significantly higher than those of the 1-month-old Smad3$^{-/-}$ mice, yet they were markedly increased compared with the 4-month-old Smad3$^{-/-}$ mice.

Relevant issues about regenerative therapy attempts include the recruitment of chondroprogenitor cells to the affected cartilage, modulation of MMPs, and the impact of the ECM on the migration of cells.[50–52] Moreover, bioactive lysophospholipids, primarily S1P, are recent additions to the list of potent mediators of tissue repair and wound healing because of their regulatory function in cell migration. S1P is released from most cells after stimulation with growth factors such as TGF-β.[15] Thus, the importance of S1P receptors for chondrocyte cell migration should be considered, although their role in OA is largely uncharacterized. On the basis of the role that S1P has in controlling cell migration in other tissues,[53] S1P and its family of receptors (previously known as EDG receptors) were investigated in Smad3$^{-/-}$ chondrocyte cells. In renal mesangial cells, several S1P receptors are expressed, including S1P$_{1-5}$, and these receptors potentially mediate mobilization of intracellular calcium, activation of the classical mitogen-activated protein kinase cascade, and cell proliferation.[38] Mandibular condylar cartilage is distinct from knee hyaline articular cartilage, and chondrocyte cells derived from the condylar cartilage of Smad3$^{-/-}$ mice were analyzed in the present study. The primary chondrocyte cells that were derived from the WT mice expressed higher levels of S1P$_3$ compared with the other S1P receptors assayed. Conversely, expression of S1P$_3$ by the primary chondrocytes derived from the Smad3$^{-/-}$ mice was significantly weaker. This difference in S1P$_3$ expression was further enhanced after TGF-β stimulation. These results are consistent with the observation that signaling through the Sphk1/S1P$_3$ axis is enhanced during the TGF-induced transdifferentiation of myoblasts into myofibroblasts.[54,55] Human articular chondrocytes also express S1P receptors in vitro,[56] and S1P-mediated cell proliferation was reported in a rat chondrocyte model.[57] However, in the latter study, a different set of S1P receptors was identified. In particular, S1P$_4$ rather than S1P$_3$ was detected.[57]

It was reported that crosstalk occurs between S1P receptors and the Smad signaling pathway, because TGF-β up-regulates both mRNA and protein levels of Sphk1 and increases Sphk1 activity in dermal fibroblasts and myofibroblasts.[58] It was also found that S1P uses the signaling of S1P receptors to stimulate the phosphorylation and activation of TGFβR kinase, thereby resulting in the phosphorylation of Smad2 and Smad3 independent of the TGF-β ligand, and the proliferation and migration of keratinocytes.[59] Thus, abrogation of Smad3 appears to prevent S1P-mediated effects, which suggests a surprising, yet essential role for Smad3 in the signaling cascade of the lysophospholipid, S1P.[59,60] By using S1P$_3$-targeting siRNA and suramin, it was further found that receptor S1P$_3$ contributes to Smad activation. Correspondingly, suramin was reported to be a selective antagonist of the S1P$_3$ receptor, in vitro.[61] Abrogation of S1P-stimulated Smad3 activation by TGFBR2-targeting siRNA also supports the hypothesis that TGF-βR II is a component of the S1P signaling cascade. However, additional studies are needed to identify the mechanistic details about the signaling of these two receptors and the identity of the cross-linked proteins that appear in Figure 6D.

Rho GTPases play a key role in coordinating the cellular responses required for cell migration.[62,63] In the present study, the Rho GTPases assayed exhibited increased levels of activity after stimulation by TGF-β. However, when primary chondrocyte cells were transfected with S1P$_3$-targeted siRNA, the activity levels of GTP-Rac1, GTP-RhoA, and GTP-Cdc42 decreased after TGF-β stimulation. Furthermore, similar results were obtained when the same set of transfected cells were grown on a 3D gel matrix and were stimulated with TGF-β (Supplemental Figure S2C).

Taken together, these findings suggest that the maintenance of chondrocyte cells, which includes the processes of cell motility and apoptosis, are regulated by crosstalk between the TGF-β/Smad3 and S1P/S1P$_3$ signaling pathways. Furthermore, Smad3/S1P$_3$ signaling in chondrocytes may play a crucial role in the cause of TMJ-OA.

Acknowledgments

Supplemental Data

References

1. McNeill C, Mohl ND, Rugh JD, Tanaka TT: Temporomandibular disorders: diagnosis, management, education, and research. J Am Dent Assoc 1990, 120:253. 255, 257 passim
2. Wang XD, Kou XX, He DQ, Zeng MM, Meng Z, Bi RY, Liu Y, Zhang JN, Gan YH, Zhou YH: Progression of cartilage degradation,

bone resorption and pain in rat temporomandibular joint osteoarthritis induced by injection of iodoacetate. PLoS One 2012, 7:e45036

3. Scrivani SJ, Keith DA, Kaban LB: Temporomandibular disorders. N Engl J Med 2008, 359:2693−2705

4. Hunter DJ: Pharmacologic therapy for osteoarthritis−the era of disease modification. Nat Rev Rheumatol 2011, 7:13−22

5. Xie L, Lin AS, Kundu K, Levenston ME, Murthy N, Guldberg RE: Quantitative imaging of cartilage and bone morphology, reactive oxygen species, and vascularization in a rodent model of osteoarthritis. Arthritis Rheum 2012, 64:1899−1908

6. Tanaka E, Detamore MS, Mercuri LG: Degenerative disorders of the temporomandibular joint: etiology, diagnosis, and treatment. J Dent Res 2008, 87:296−307

7. Embree M, Ono M, Kilts T, Walker D, Langguth J, Mao J, Bi Y, Barth JL, Young M: Role of subchondral bone during early-stage experimental TMJ osteoarthritis. J Dent Res 2011, 90:1331−1338

8. Jiao K, Niu LN, Wang MQ, Dai J, Yu SB, Liu XD, Wang J: Subchondral bone loss following orthodontically induced cartilage degradation in the mandibular condyles of rats. Bone 2011, 48:362−371

9. Zhang J, Jiao K, Zhang M, Zhou T, Liu XD, Yu SB, Lu L, Jing L, Yang T, Zhang Y, Chen D, Wang MQ: Occlusal effects on longitudinal bone alterations of the temporomandibular joint. J Dent Res 2013, 92:253−259

10. Shen G, Darendeliler MA: The adaptive remodeling of condylar cartilage−a transition from chondrogenesis to osteogenesis. J Dent Res 2005, 84:691−699

11. Bismar H, Kloppinger T, Schuster EM, Balbach S, Diel I, Ziegler R, Pfeilschifter J: Transforming growth factor beta (TGF-beta) levels in the conditioned media of human bone cells: relationship to donor age, bone volume, and concentration of TGF-beta in human bone matrix in vivo. Bone 1999, 24:565−569

12. Janssens K, ten Dijke P, Janssens S, Van Hul W: Transforming growth factor-beta1 to the bone. Endocr Rev 2005, 26:743−774

13. Tang Y, Wu X, Lei W, Pang L, Wan C, Shi Z, Zhao L, Nagy TR, Peng X, Hu J, Feng X, Van Hul W, Wan M, Cao X: TGF-beta1-induced migration of bone mesenchymal stem cells couples bone resorption with formation. Nat Med 2009, 15:757−765

14. Yang X, Chen L, Xu X, Li C, Huang C, Deng CX: TGF-beta/Smad3 signals repress chondrocyte hypertrophic differentiation and are required for maintaining articular cartilage. J Cell Biol 2001, 153:35−46

15. Watterson KR, Lanning DA, Diegelmann RF, Spiegel S: Regulation of fibroblast functions by lysophospholipid mediators: potential roles in wound healing. Wound Repair Regen 2007, 15:607−616

16. Alvarez SE, Milstien S, Spiegel S: Autocrine and paracrine roles of sphingosine-1-phosphate. Trends Endocrinol Metab 2007, 18:300−307

17. Wang F, Van Brocklyn JR, Hobson JP, Movafagh S, Zukowska-Grojec Z, Milstien S, Spiegel S: Sphingosine 1-phosphate stimulates cell migration through a G(i)-coupled cell surface receptor. Potential involvement in angiogenesis. J Biol Chem 1999, 274:35343−35350

18. Liu Y, Wada R, Yamashita T, Mi Y, Deng CX, Hobson JP, Rosenfeldt HM, Nava VE, Chae SS, Lee MJ, Liu CH, Hla T, Spiegel S, Proia RL: Edg-1, the G protein-coupled receptor for sphingosine-1-phosphate, is essential for vascular maturation. J Clin Invest 2000, 106:951−961

19. Vogler R, Sauer B, Kim DS, Schafer-Korting M, Kleuser B: Sphingosine-1-phosphate and its potentially paradoxical effects on critical parameters of cutaneous wound healing. J Invest Dermatol 2003, 120:693−700

20. Yang X, Letterio JJ, Lechleider RJ, Chen L, Hayman R, Gu H, Roberts AB, Deng C: Targeted disruption of SMAD3 results in impaired mucosal immunity and diminished T cell responsiveness to TGF-beta. EMBO J 1999, 18:1280−1291

21. Yokozeki M, Afanador E, Nishi M, Kaneko K, Shimokawa H, Yokote K, Deng C, Tsuchida K, Sugino H, Moriyama K: Smad3 is

required for enamel biomineralization. Biochem Biophys Res Commun 2003, 305:684−690

22. Xu L, Flahiff CM, Waldman BA, Wu D, Olsen BR, Setton LA, Li Y: Osteoarthritis-like changes and decreased mechanical function of articular cartilage in the joints of mice with the chondrodysplasia gene (cho). Arthritis Rheum 2003, 48:2509−2518

23. Embree MC, Kilts TM, Ono M, Inkson CA, Syed-Picard F, Karsdal MA, Oldberg A, Bi Y, Young MF: Biglycan and fibromodulin have essential roles in regulating chondrogenesis and extracellular matrix turnover in temporomandibular joint osteoarthritis. Am J Pathol 2010, 176:812−826

24. Salvat C, Pigenet A, Humbert L, Berenbaum F, Thirion S: Immature murine articular chondrocytes in primary culture: a new tool for investigating cartilage. Osteoarthritis Cartilage 2005, 13:243−249

25. Yasui T, Kadono Y, Nakamura M, Oshima Y, Matsumoto T, Masuda H, Hirose J, Omata Y, Yasuda H, Imamura T, Nakamura K, Tanaka S: Regulation of RANKL-induced osteoclastogenesis by TGF-beta through molecular interaction between Smad3 and Traf6. J Bone Miner Res 2011, 26:1447−1456

26. Sharif M, Whitehouse A, Sharman P, Perry M, Adams M: Increased apoptosis in human osteoarthritic cartilage corresponds to reduced cell density and expression of caspase-3. Arthritis Rheum 2004, 50:507−515

27. Thomas CM, Fuller CJ, Whittles CE, Sharif M: Chondrocyte death by apoptosis is associated with cartilage matrix degradation. Osteoarthritis Cartilage 2007, 15:27−34

28. Huser CA, Peacock M, Davies ME: Inhibition of caspase-9 reduces chondrocyte apoptosis and proteoglycan loss following mechanical trauma. Osteoarthritis Cartilage 2006, 14:1002−1010

29. Kronenberg HM: Developmental regulation of the growth plate. Nature 2003, 423:332−336

30. Rivera J, Proia RL, Olivera A: The alliance of sphingosine-1-phosphate and its receptors in immunity. Nat Rev Immunol 2008, 8:753−763

31. de Crombrugghe B, Lefebvre V, Behringer RR, Bi W, Murakami S, Huang W: Transcriptional mechanisms of chondrocyte differentiation. Matrix Biol 2000, 19:389−394

32. Li F, Lu Y, Ding M, Napierala D, Abbassi S, Chen Y, Duan X, Wang S, Lee B, Zheng Q: Runx2 contributes to murine Col10a1 gene regulation through direct interaction with its cis-enhancer. J Bone Miner Res 2011, 26:2899−2910

33. Zheng Q, Zhou G, Morello R, Chen Y, Garcia-Rojas X, Lee B: Type X collagen gene regulation by Runx2 contributes directly to its hypertrophic chondrocyte-specific expression in vivo. J Cell Biol 2003, 162:833−842

34. Cucchiarini M, Thurn T, Weimer A, Kohn D, Terwilliger EF, Madry H: Restoration of the extracellular matrix in human osteoarthritic articular cartilage by overexpression of the transcription factor SOX9. Arthritis Rheum 2007, 56:158−167

35. von der Mark K, Kirsch T, Nerlich A, Kuss A, Weseloh G, Gluckert K, Stoss H: Type X collagen synthesis in human osteoarthritic cartilage. Indication of chondrocyte hypertrophy. Arthritis Rheum 1992, 35:806−811

36. Fuerst M, Bertrand J, Lammers L, Dreier R, Echtermeyer F, Nitschke Y, Rutsch F, Schafer FK, Niggemeyer O, Steinhagen J, Lohmann CH, Pap T, Ruther W: Calcification of articular cartilage in human osteoarthritis. Arthritis Rheum 2009, 60:2694−2703

37. Zhen G, Wen C, Jia X, Li Y, Crane JL, Mears SC, Askin FB, Frassica FJ, Chang W, Yao J, Carrino JA, Cosgarea A, Artemov D, Chen Q, Zhao Z, Zhou X, Riley L, Sponseller P, Wan M, Lu WW, Cao X: Inhibition of TGF-beta signaling in mesenchymal stem cells of subchondral bone attenuates osteoarthritis. Nat Med 2013, 19:704−712

38. Katsuma S, Hada Y, Ueda T, Shiojima S, Hirasawa A, Tanoue A, Takagaki K, Ohgi T, Yano J, Tsujimoto G: Signalling mechanisms in sphingosine 1-phosphate-promoted mesangial cell proliferation. Genes Cells 2002, 7:1217−1230

39. Datto MB, Frederick JP, Pan L, Borton AJ, Zhuang Y, Wang XF: Targeted disruption of Smad3 reveals an essential role in transforming growth factor beta-mediated signal transduction. Mol Cell Biol 1999, 19:2495−2504

40. Ashcroft GS, Yang X, Glick AB, Weinstein M, Letterio JL, Mizel DE, Anzano M, Greenwell-Wild T, Wahl SM, Deng C, Roberts AB: Mice lacking Smad3 show accelerated wound healing and an impaired local inflammatory response. Nat Cell Biol 1999, 1:260−266

41. Zhu Y, Richardson JA, Parada LF, Graff JM: Smad3 mutant mice develop metastatic colorectal cancer. Cell 1998, 94:703−714

42. Schiller M, Javelaud D, Mauviel A: TGF-beta-induced SMAD signaling and gene regulation: consequences for extracellular matrix remodeling and wound healing. J Dermatol Sci 2004, 35:83−92

43. Kapoor M, Martel-Pelletier J, Lajeunesse D, Pelletier JP, Fahmi H: Role of proinflammatory cytokines in the pathophysiology of osteoarthritis. Nat Rev Rheumatol 2011, 7:33−42

44. Pelletier JP, Boileau C, Brunet J, Boily M, Lajeunesse D, Reboul P, Laufer S, Martel-Pelletier J: The inhibition of subchondral bone resorption in the early phase of experimental dog osteoarthritis by licofelone is associated with a reduction in the synthesis of MMP-13 and cathepsin K. Bone 2004, 34:527−538

45. Zhu M, Tang D, Wu Q, Hao S, Chen M, Xie C, Rosier RN, O'Keefe RJ, Zuscik M, Chen D: Activation of beta-catenin signaling in articular chondrocytes leads to osteoarthritis-like phenotype in adult beta-catenin conditional activation mice. J Bone Miner Res 2009, 24:12−21

46. Chen CG, Thuillier D, Chin EN, Alliston T: Chondrocyte-intrinsic Smad3 represses Runx2-inducible matrix metalloproteinase 13 expression to maintain articular cartilage and prevent osteoarthritis. Arthritis Rheum 2012, 64:3278−3289

47. van de Laar IM, Oldenburg RA, Pals G, Roos-Hesselink JW, de Graaf BM, Verhagen JM, Hoedemaekers YM, Willemsen R, Severijnen LA, Venselaar H, Vriend G, Pattynama PM, Collee M, Majoor-Krakauer D, Poldermans D, Frohn-Mulder IM, Micha D, Timmermans J, Hilhorst-Hofstee Y, Bierma-Zeinstra SM, Willems PJ, Kros JM, Oei EH, Oostra BA, Wessels MW, Bertoli-Avella AM: Mutations in SMAD3 cause a syndromic form of aortic aneurysms and dissections with early-onset osteoarthritis. Nat Genet 2011, 43:121−126

48. Jiao K, Zhang M, Niu L, Yu S, Zhen G, Xian L, Yu B, Yang K, Liu P, Cao X, Wang M: Overexpressed TGF-beta in subchondral bone leads to mandibular condyle degradation. J Dent Res 2014, 93:140−147

49. Kim HA, Suh DI, Song YW: Relationship between chondrocyte apoptosis and matrix depletion in human articular cartilage. J Rheumatol 2001, 28:2038−2045

50. Koelling S, Kruegel J, Irmer M, Path JR, Sadowski B, Miro X, Miosge N: Migratory chondrogenic progenitor cells from repair tissue during the later stages of human osteoarthritis. Cell Stem Cell 2009, 4:324−335

51. Gerter R, Kruegel J, Miosge N: New insights into cartilage repair - the role of migratory progenitor cells in osteoarthritis. Matrix Biol 2012, 31:206−213

52. Seol D, McCabe DJ, Choe H, Zheng H, Yu Y, Jang K, Walter MW, Lehman AD, Ding L, Buckwalter JA, Martin JA: Chondrogenic progenitor cells respond to cartilage injury. Arthritis Rheum 2012, 64:3626−3637

53. Ishii M, Egen JG, Klauschen F, Meier-Schellersheim M, Saeki Y, Vacher J, Proia RL, Germain RN: Sphingosine-1-phosphate mobilizes osteoclast precursors and regulates bone homeostasis. Nature 2009, 458:524−528

54. Cencetti F, Bernacchioni C, Nincheri P, Donati C, Bruni P: Transforming growth factor-beta1 induces transdifferentiation of myoblasts into myofibroblasts via up-regulation of sphingosine kinase-1/S1P3 axis. Mol Biol Cell 2010, 21:1111−1124

55. Keller CD, Rivera Gil P, Tolle M, van der Giet M, Chun J, Radeke HH, Schafer-Korting M, Kleuser B: Immunomodulator FTY720 induces myofibroblast differentiation via the lysophospholipid receptor S1P3 and Smad3 signaling. Am J Pathol 2007, 170:281−292

56. Stradner MH, Hermann J, Angerer H, Setznagl D, Sunk I, Windhager R, Graninger WB: Spingosine-1-phosphate stimulates proliferation and counteracts interleukin-1 induced nitric oxide formation in articular chondrocytes. Osteoarthritis Cartilage 2008, 16:305−311

57. Kim MK, Lee HY, Kwak JY, Park JI, Yun J, Bae YS: Sphingosine-1-phosphate stimulates rat primary chondrocyte proliferation. Biochem Biophys Res Commun 2006, 345:67−73

58. Yamanaka M, Shegogue D, Pei H, Bu S, Bielawska A, Bielawski J, Pettus B, Hannun YA, Obeid L, Trojanowska M: Sphingosine kinase 1 (SPHK1) is induced by transforming growth factor-beta and mediates TIMP-1 up-regulation. J Biol Chem 2004, 279:53994−54001

59. Sauer B, Vogler R, von Wenckstern H, Fujii M, Anzano MB, Glick AB, Schafer-Korting M, Roberts AB, Kleuser B: Involvement of Smad signaling in sphingosine 1-phosphate-mediated biological responses of keratinocytes. J Biol Chem 2004, 279:38471−38479

60. Radeke HH, von Wenckstern H, Stoidtner K, Sauer B, Hammer S, Kleuser B: Overlapping signaling pathways of sphingosine 1-phosphate and TGF-beta in the murine Langerhans cell line XS52. J Immunol 2005, 174:2778−2786

61. Ancellin N, Hla T: Differential pharmacological properties and signal transduction of the sphingosine 1-phosphate receptors EDG-1, EDG-3, and EDG-5. J Biol Chem 1999, 274:18997−19002

62. Ridley AJ: Rho GTPases and cell migration. J Cell Sci 2001, 114:2713−2722

63. Raftopoulou M, Hall A: Cell migration: Rho GTPases lead the way. Dev Biol 2004, 265:23−32

Supplemental Figure S1   Immunohistochemical analysis of mandibular articular cartilage obtained from 1M WT and *Smad3*$^{-/-}$ littermates. **A:** Expression levels of phosphorylated Smad3, Col2a1, and aggrecan were detected. **B:** Expression levels of MMP-13 and MMP-9 were detected by immunohistochemistry. **C:** Expression levels of caspase-3 and caspase-9 were detected. For the immunohistochemical analysis of negative controls, primary antibodies were replaced with IgG to confirm the specificity of the staining. *n* = 5 mice from each group. Scale bar = 100 μm. Col2a1, type II collagen; MMP, matrix metallopeptidase; WT, wild-type; 1M, 1-month-old mice.

Supplemental Figure S2   **A:** Growth of mouse chondroprogenitor ATDC cells in a 3D culture matrix enhances TGF-β—mediated Rho-GTP activity. ATDC5 cells were cultured in 3D Matrigel or on 2D culture dishes in the presence of 5 ng/mL TGF-β1 for 0 to 30 minutes. The corresponding total cell lysates (50 μg) were subjected to Western blot analysis to detect expression of p-Smad3. GAPDH was used as an internal control. Levels of Rac1-GTP and RhoA-GTP activities were measured by a pull-down assay kit, with total Rac1 and RhoA immunoblotted in lysates. **B:** ATDC5 cells that were transfected with *Smad3*-targeted siRNA and cultured on 3D Matrigel were incubated with 5 ng/mL TGF-β1 for 0 to 30 minutes. ATDC5 cell lysates were then assayed for levels of Rac1-GTP, RhoA-GTP, and Cdc42-GTP activities by using a pull-down assay kit. Total cell lysates (50 μg) were also subjected to Western blot analysis to detect expression of total Rac1, total RhoA, and total Cdc42. **C:** Primary chondrocytes transfected with *S1P₃*-targeted siRNA were cultured on 3D Matrigel and then were incubated with 5 ng/mL TGF-β1 for 0 to 30 minutes. Total cell lysates were assayed for levels of Rac1-GTP, RhoA-GTP, and Cdc42-GTP activities by using a pull-down assay kit. Total cell lysates (50 μg) were also subjected to Western blot analysis to detect expression of total Rac1, total RhoA, and total Cdc42. *n* = 2 independent experiments. GAPDH, glyceraldehyde 3-phosphate dehydrogenase; S1P₃, sphingosine 1-phosphate receptor 3; TGF, transforming growth factor; 2D, two-dimensional; 3D, three-dimensional.

Supplemental Figure S3   **A:** Calvarial osteoblast and mandibular primary chondrocyte cells were isolated from WT mice and were subjected to real-time PCR analysis with the use of primers specific for Sox9, Col2a1, osteocalcin, Col1a1, and GAPDH. **B:** Mandibular primary chondrocyte cells were isolated from WT mice and were stained with Alcian Blue. Immunocytochemistry also detected Col2a1 (green), one of the markers of the chondrogenic lineage. Nuclei were stained with DAPI (blue). **C:** Mandibular primary chondrocytes were isolated from 4-month-old WT and *Smad3*$^{-/-}$ mice and subjected to real-time PCR analysis with the use of primers specific for Sox9, Col10a1, and GAPDH. **D:** Immunoblot analysis of mandibular primary chondrocyte cells isolated from 4-month-old WT and *Smad3*$^{-/-}$ littermates. Expression levels of Sox9 and type X collagen were detected in the articular cartilage. Detection of β-actin was used as an internal control. **E:** Immunohistochemical analysis of type X collagen in mandibular articular cartilage obtained from 4-month-old WT and *Smad3*$^{-/-}$ mice. As a negative control, mandibular articular cartilage obtained from 4-month-old *Smad3*$^{-/-}$ mice were stained with rabbit IgG (isotype control). Data are expressed as means ± SD (**A**). *n* = 3 from three independent experiments (**A** and **B**); *n* = 5 mice per group of three independent experiments (**C**); *n* = 2 independent experiments (**D**); *n* = 3 mice from each group (**E**). Scale bar = 100 μm. *P < 0.05, **P < 0.01. Col1a1, type I collagen; Col2a1, type II collagen; GAPDH, glyceraldehyde 3-phosphate dehydrogenase; WT, wild-type.